

Thermomagnonic spin transfer and Peltier effects in insulating magnets

ALEXEY A. KOVALEV¹ and YAROSLAV TSERKOVNYAK²

¹ *Department of Physics and Astronomy, University of California, Riverside, California 92521, USA*

² *Department of Physics and Astronomy, University of California, Los Angeles, California 90095, USA*

PACS 72.20.Pa – Thermoelectric and thermomagnetic effects

PACS 75.30.Ds – Spin waves

PACS 72.20.My – Galvanomagnetic and other magnetotransport effects

Abstract – We study the coupled magnon energy transport and collective magnetization dynamics in ferromagnets with magnetic textures. By constructing a phenomenological theory based on irreversible thermodynamics, we describe motion of domain walls by thermal gradients and generation of heat flows by magnetization dynamics. From microscopic description based on magnon kinetics, we estimate the transport coefficients and analyze the feasibility of energy-related applications in insulating ferromagnets, such as yttrium iron garnet and europium oxide.

Introduction. – Most electronic devices rely on charge current flows controlled by applied voltages. It has been realized that spin-polarized charge flows can also be induced by fictitious electromagnetic fields due to magnetic texture dynamics [1, 2]. Recently, the possibility of employing spin in electronic logic devices has also been suggested [3]. However, since it may be energy-costly to create and maintain spin imbalances electrically, the fictitious electromagnetic fields induced by magnetic textures may become useful for such applications. Reciprocal motion of magnetic textures due to weak charge-current-induced spin transfer is governed by dissipative torques (so-called “ β terms”) [4–8] associated with microscopic spin misalignments, which will also play an important role in our study.

The spin flows are known to coexist with heat flows in transition metals, where both fluxes can be effectively driven by the moving magnetic texture [9, 10]. Similar effects have also been studied in magnetic semiconductors [11]. The reciprocal action of the spin-transfer torque (STT) on the magnetization [12] is extremely important for applications, e.g., spin-transfer torque memory and nonvolatile logic. Spin torques due to pure spin currents have been observed in experiments on spin pumping by magnetic precession [13] or spin Hall effect along magnetic insulator surface [14]. Thermal spin torques have been studied in magnetic nanopillars [15] with recent developments suggesting that they can be more efficient compared to electrically generated spin torques [16].

Spin and heat currents can be also induced in insulating systems, such as yttrium iron garnet (YIG), by the external microwave magnetic field [14]. Alternatively, the temperature gradient can lead to a spin imbalance by the spin Seebeck effect [17]. The heat currents accompanying the spin-wave (magnon) flows in an insulating ferromagnet $\text{Lu}_2\text{V}_2\text{O}_7$ have been used to detect the magnon Hall effect [18]. Here, we are interested in the possibility to use fictitious electromagnetic fields induced by magnetic textures to control magnon spin flows in a manner similar to spin-polarized charge currents.

In this Letter, we study interplay between magnon-carried heat and spin currents and magnetic texture dynamics in ferromagnets by formulating a hydrodynamic phenomenological description of magnonic and thermal currents coupled to geometric gauge fields (the charge currents are ignored in our description but can be readily reintroduced in case of metals [9]). By considering dissipative corrections (“ β terms”), we show that they play an important role as they do in electronic systems, enabling domain-wall (DW) motion below the Walker breakdown and heat pumping [9]. To justify our phenomenology, we also formulate a ground-up kinetic description of thermal magnons, which allows us to identify the phenomenological coefficients entering the hydrodynamic theory. The DW motion and heat pumping are studied in YIG and EuO and the feasibility of energy-related applications is discussed.

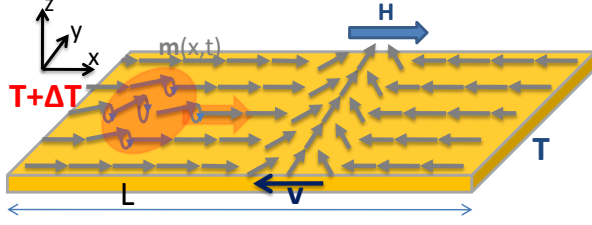


Fig. 1: The magnon current induced by temperature gradient exerts spin torque on the magnetization, according to the conservation of angular momentum, which can lead to a domain-wall motion. The inverse effect of magnon current induced by magnetization motion is also possible, wherein the collective magnetic texture $\mathbf{m}(x, t)$ is controlled by effective field \mathbf{H} .

Phenomenological description of magnonic and thermal currents in textured magnets. – We construct a general phenomenological description of magnonic and thermal currents in textured magnets (Fig. 1) based on several thermodynamic variables such as the direction of the slow (averaged over the magnonic excitations) spin density \mathbf{m}_s (the label s is dropped in this section), density of magnons ρ and density of energy ρ_U . The ferromagnet can be taken out of equilibrium by applying temperature, chemical potential and magnetization gradients, while the equilibrium state can be topologically nontrivial, e.g., a magnetic DW or vortex. In the absence of bias, the ferromagnet would then evolve back towards equilibrium according to the equations of motion. Following the standard route, we identify thermodynamic variables x_k and their conjugates (generalized forces) $X_k = \partial\mathcal{S}/\partial x_k$ by writing the entropy \mathcal{S} production in the following form:

$$\dot{\mathcal{S}} = \sum X_k \dot{x}_k. \quad (1)$$

The local conservation laws of energy and (approximately) magnon number provide us with continuity relations: $\dot{\rho} = -\nabla \cdot \mathbf{j} - (\rho - \rho_0)/\tau_\alpha$ and $\dot{\rho}_U = -\nabla \cdot \mathbf{j}_U$, where we introduced the magnon-number (\mathbf{j}) and energy (\mathbf{j}_U) current densities, and τ_α corresponds to the life time of magnons (that are in excess of a local-equilibrium value ρ_0). We now write the rate of the entropy production in a standard manner [19]:

$$\dot{\mathcal{S}} = - \int d^3\mathbf{r} \frac{\nabla \cdot \mathbf{j}_U + \mu \dot{\rho} + \mathcal{H} \cdot \dot{\mathbf{m}}}{T}, \quad (2)$$

where the conjugate force corresponding to the magnetic (spin-density) direction \mathbf{m} is defined as $-\delta_{\mathbf{m}}\mathcal{S}|_{\mathbf{j}_U(\mathbf{j})=0} = \mathcal{H}/T$. By straightforward manipulation, in which we introduce the modified energy current $\mathbf{j}_q = \mathbf{j}_U - \mu \mathbf{j}$, we arrive at the following equation for the rate of the entropy production:

$$\dot{\mathcal{S}} = \int d^3\mathbf{r} \left[\nabla \cdot \left(\frac{1}{T} \right) \mathbf{j}_q - \frac{\nabla \mu}{T} \cdot \mathbf{j} - \frac{\mathcal{H}}{T} \cdot \dot{\mathbf{m}} \right], \quad (3)$$

where in Eq. (2) we integrated the term involving \mathbf{j}_q by parts, used the continuity equations and disregarded

magnon decay $\propto (\rho - \rho_0)/\tau_\alpha$. The latter is justified when either (i) the number of magnons is (to a good approximation) conserved, which means that the relevant size of the system is smaller than the magnon decay length corresponding to τ_α , or (ii) no build-up of magnons takes place due to fast relaxation or uniform current generation (thus $\rho \approx \rho_0$). The forces conjugate to the fluxes can be immediately identified as $-\partial_{\mathbf{j}_q} \dot{\mathcal{S}}|_{\mathbf{m}, \mathbf{j}=0} = -\nabla(1/T)$ and $-\partial_{\mathbf{j}} \dot{\mathcal{S}}|_{\mathbf{m}, \mathbf{j}_q=0} = \nabla \mu/T$. Formally, Eq. (3) is identical to the one used in Ref. [9], which suggests similarities between phenomenological theories for magnons and electrons.

We now relate the currents \mathbf{j} and \mathbf{j}_q as well as the time derivative of the collective spin-density direction, $\dot{\mathbf{m}}$, to the thermodynamic conjugates via kinetic coefficients. The kinetic coefficients can be further identified by noting that the currents \mathbf{j} and \mathbf{j}_q are determined by the chemical potential and temperature gradients as well as the magnetic texture dynamics, which exerts fictitious Berry phase gauge fields on the magnons. By assuming the spin-rotational symmetry of the magnetic texture and isotropy in real space, we obtain the magnon and energy current gradient expansion:

$$\begin{aligned} -\partial_i \mu &= \Upsilon_{ik} j_k + \Pi_{ik} \partial_k T/T - p (\mathbf{m} \times \partial_i \mathbf{m} + \beta \partial_i \mathbf{m}) \cdot \dot{\mathbf{m}}, \\ (j_q^h)_i &= \Pi_{ik}^T j_k - \kappa_{ik} \partial_k T - p_1 (\mathbf{m} \times \partial_i \mathbf{m} + \beta_1 \partial_i \mathbf{m}) \cdot \dot{\mathbf{m}}, \\ \mathfrak{s}(1 + \alpha \mathbf{m} \times) \dot{\mathbf{m}} + \mathbf{m} \times \mathbf{H}_{\text{eff}} &= p [\partial_i \mathbf{m} + \beta \mathbf{m} \times \partial_i \mathbf{m}] j_i \\ &\quad + p_1 [\partial_i \mathbf{m} + \beta_1 \mathbf{m} \times \partial_i \mathbf{m}] \partial_i T/T, \end{aligned} \quad (4)$$

where the equation for the magnon current has been inverted, Υ_{ik} , Π_{ik} and κ_{ik} are the resistivity, Peltier and thermal conductivity tensors, respectively, which are in general temperature and texture dependent ($p_1 \beta_1$ has to be treated as one coefficient when $p_1 = 0$) and the LLG part has been completed by employing the Onsager reciprocity principle. The heat current in Eq. (3) includes the contribution from the magnetic energy contained in the texture \mathbf{j}_q^t (e.g., exchange energy flow accompanying the DW motion). In situations when the texture energy contribution can be separated from the “real” heat current, we choose to subtract this contribution, i.e., $\mathbf{j}_q^h = \mathbf{j}_q - \mathbf{j}_q^t$ in Eq. (4). By invoking the time reversal argument, one can show that the gradient expansion of the texture energy contribution has the form $(j_q^t)_i = p^t \beta^t \partial_i \mathbf{m} \cdot \dot{\mathbf{m}}$. Equation (3) can now be reformulated using the “pure” heat current $\mathbf{j}_q^h = \mathbf{j}_q - \mathbf{j}_q^t$ where as it follows from Eq. (3) the effective field has to be redefined as $\mathbf{H}_{\text{eff}} = \mathcal{H} - p^t \beta^t \partial_i \mathbf{m} \partial_i (1/T)$. The new notations allow for more natural separation of the magnetic and heat degrees of freedom, e.g., in the simplest approximation one can assume that even in an out-of-equilibrium situation, when $\partial_i T \neq 0$ and $\partial_i \mu \neq 0$, \mathbf{H}_{eff} depends only on the instantaneous texture $\mathbf{m}(\mathbf{r}, t)$. In general, we may expand \mathbf{H}_{eff} phenomenologically in terms of small $\partial_i T$ and $\partial_i \mu$. The form of Eqs. (4) is the same for both sets of variables ($\mathbf{j}_q^h \leftrightarrow \mathbf{j}_q$, $\mathbf{H}_{\text{eff}} \leftrightarrow \mathcal{H}$) but the kinetic coefficients are different. The rest of the paper relies on equations written for $(\mathbf{j}_q^h, \mathbf{H}_{\text{eff}})$. Note that in Ref. [9] it was implied that the latter set of variables had been used.

The tensors Υ_{ik} , Π_{ik} and κ_{ik} can depend on temperature and texture, i.e., to the leading order, as

$$\begin{aligned} \kappa_{ik}(\Pi_{ik}, \Upsilon_{ik}) = & \delta_{ik} [\kappa(\Pi, \Upsilon) + \eta_{\kappa(\Pi, \Upsilon)}(\partial_l \mathbf{m})^2] \\ & + \eta'_{\kappa(\Pi, \Upsilon)} \partial_i \mathbf{m} \cdot \partial_k \mathbf{m} + b_{\kappa(\Pi, \Upsilon)} \mathbf{m} \cdot (\partial_i \mathbf{m} \times \partial_k \mathbf{m}). \end{aligned}$$

Equations (4) should also be applicable to magnetization dynamics in the presence of charge currents (the magnon current has to be replaced by the charge current) as discussed in Ref. [9]. These equations should describe such fictitious-field induced effects on magnons (electrons) as the Hall effect (coefficient b_Υ), the Etingshausen effect (coefficient b_Π/κ), the Nernst effect (coefficient b_Π/T), and the Righi-Leduc effect (coefficient b_Π/Π).

The gradient expansion in Eq. (4) assumes short magnon wavelength compared to the characteristic textures length scale. In YIG, for example, the former is ~ 1 nm at room temperature, which should not pose a serious constraint for such adiabatic description.

Bottom up construction of phenomenology for thermal magnons. – Since we concentrate on the low temperature limit (on the scale set by the Curie temperature) the LLG phenomenology remains reliable microscopically. Coarse graining thermal fluctuations thereof would however lead to modified effective quantities (such as spin density and stiffness constant). Consider a ferromagnet with space- and time-dependent spin density $s\mathbf{m}(\mathbf{r}, t)$ with magnitude s saturated at a constant value and direction described by a unit vector $\mathbf{m}(\mathbf{r}, t)$. The spin density is assumed to have two components – fast and slow where the slow component slowly varies in space and time with much larger characteristic scales compared to the fast component. The effect of topological gauge fields due to magnetic textures of the slow component can be captured by considering the Lagrangian [20]:

$$\mathcal{L} = \int d^3\mathbf{r} [\mathbf{D}(\mathbf{m}) \cdot \dot{\mathbf{m}} - E(\mathbf{m}, \partial_\alpha \mathbf{m})], \quad (5)$$

where $\mathbf{D}(\mathbf{m}) = s[\mathbf{n} \times \mathbf{m}]/(1 + \mathbf{m} \cdot \mathbf{n})$ is the vector potential of the Wess-Zumino action with an arbitrary \mathbf{n} pointing along the Dirac string, $E(\mathbf{m}, \partial_\alpha \mathbf{m})$ is the magnetic energy density describing the exchange energy as well as the external and anisotropy fields. Equation (5) leads to the Landau-Lifshitz (LL) equation $s\dot{\mathbf{m}} - \mathbf{m} \times \delta_{\mathbf{m}} E = 0$. We assume in our description that the magnetic energy density is given by $E/M_s = A(\partial_\alpha \mathbf{m})^2 - \mathbf{m} \cdot \mathbf{H}_m/2 - \mathbf{m} \cdot \mathbf{H}$ where A is the exchange stiffness, M_s is the saturation magnetization, \mathbf{H}_m describes magnetostatic and magnetocrystalline anisotropies (largely ignored in our description of thermal magnons at sufficiently high temperatures; but would otherwise suppress the fictitious forces acting on magnons [21]), and \mathbf{H} is the external magnetic field. For the purpose of deriving the equations of motion, we use a coordinate transformation after which the z -axis points along the spin density of the slow dynamics. In the new coordinate system, small excitations will only have m_x and m_y components.

Equations for the slow dynamics in the original (lab) frame can be obtained from the LL equation with a dissipative term by coarse-graining over fast variables, i.e., $s \langle \mathbf{m} \rangle_{\text{fast}} = \mathbf{s}(\mathbf{r}, t)\mathbf{m}_s$ with the final result:

$$\begin{aligned} s\dot{\mathbf{m}}_s + \mathbf{m}_s \times \mathbf{H}_{\text{eff}}^s = & \hbar \partial_\alpha \mathbf{j}_\alpha + \alpha \mathbf{m}_s \times (\mathbf{m}_s \times \mathbf{H}_{\text{eff}}^s) \\ & - \hbar(\alpha - \beta) \mathbf{m}_s \times (\partial_\alpha \mathbf{j}_\alpha), \end{aligned} \quad (6)$$

where the l.h.s. is written for the magnon-averaged spin density \mathbf{s} , \mathbf{m} and \mathbf{m}_s are unit vectors, i.e., $\mathbf{m}_f = \mathbf{m} - (\mathbf{s}/s)\mathbf{m}_s$ corresponds to the fast dynamics, the spin current density $\hbar \mathbf{j}_\alpha = M_s A [\mathbf{m}_f \times \partial_\alpha \mathbf{m}_f]$, $\mathbf{H}_{\text{eff}}^s = -\delta_{\mathbf{m}_s} E\{(\mathbf{s}/s)\mathbf{m}_s, \partial_\alpha[(\mathbf{s}/s)\mathbf{m}_s]\}$ is the effective field of the slow dynamics and β accounts for the fact that magnons misalign with the direction of the slow dynamics [4]. Note that Eq. (6) assumes short magnon wavelengths compared to the slow texture length scale. By multiplying Eq. (6) by $1 + \alpha \mathbf{m}_s \times$ from the left and using an approximation $\partial_\alpha \mathbf{j}_\alpha \approx (j_i \partial_i) \mathbf{m}_s$ (j_i corresponds to the magnon number flux) which is true for slowly varying textures, we recover the Landau-Lifshitz-Gilbert (LLG) equation:

$$\mathbf{s}(1 + \alpha \mathbf{m}_s \times) \dot{\mathbf{m}}_s + \mathbf{m}_s \times \mathbf{H}_{\text{eff}}^s = \hbar [1 + \beta \mathbf{m}_s \times] (j_i \partial_i) \mathbf{m}_s, \quad (7)$$

In order to describe small excitations (spin waves) in the coordinates with the z -axis pointing along the slow dynamics, we introduce 3×3 rotation matrix $\hat{R} = \exp(\psi \hat{J}_z) \exp(\theta \hat{J}_y) \exp(\phi \hat{J}_z)$ with \hat{J}_α being the 3×3 matrix describing infinitesimal rotation along the axis with index α . In the new coordinates, we have $\mathbf{m} \rightarrow \mathbf{m}' = \hat{R} \mathbf{m}$ and $\partial_\mu \rightarrow (\partial_\mu - \hat{A}_\mu)$ with $\hat{A}_\mu = (\partial_\mu \hat{R}) \hat{R}^{-1}$ (the index $\mu = 0, \dots, 3$ denotes the time and space coordinates). Since the matrix \hat{A}_μ is skew-symmetric, we can introduce a vector \mathcal{A}_μ so that $\hat{A}_\mu \mathbf{m} = \mathcal{A}_\mu \times \mathbf{m}$. In a specific gauge with the Euler angle $\psi = 0$, the elements of \mathcal{A}_μ become $\mathcal{A}_\mu = (-\sin \theta \partial_\mu \phi, \partial_\mu \theta, \cos \theta \partial_\mu \phi)$. The equation describing spin waves follows from the LL equation subject to the coordinate transformation:

$$i(\partial_t - i\mathcal{A}_0^z) m_+ = A(\partial_\alpha/i - \mathcal{A}_\alpha^z)^2 m_+ + V(\mathbf{r}) m_+. \quad (8)$$

Here $V(\mathbf{r}) = \mathbf{m}_s \cdot \mathbf{H}/s - A(\mathcal{A}_x^2 + \mathcal{A}_y^2)/2$ is the effective potential and \mathbf{m}_s is the unit vector along the spin density of the slow dynamics. Second order terms in the effective potential $\sim \mathcal{A}_\mu^2$ are not treated systematically as there are similar corrections that lead to the coupling between the circular components of spin wave $m_\pm = m'_x(\mathbf{r}, t) \pm im'_y(\mathbf{r}, t)$ where $m'_{x(y)}(\mathbf{r}, t)$ describes the transverse excitations in the transformed coordinates with the z axis pointing along the direction of \mathbf{m}_s (in the absence of texture $m_+ \sim \exp(i\mathbf{q}\mathbf{r} + i\omega_q t)$). We omitted damping terms for the case when the region of interest is smaller than the length corresponding to the lifetime of spin waves. The coupling between the circular components of spin wave due to anisotropies is disregarded since we assume that the exchange effects dominate. By quantizing spin waves, we introduce the field operator $\psi = \sqrt{s/2\hbar^2} m_+ = \sqrt{1/\hbar} \sum_{\mathbf{q}} b_{\mathbf{q}} e^{i\mathbf{q}\mathbf{r}}$ corresponding to m_+ and describing magnons with spectrum

$\omega_q = V(\mathbf{r}) + Aq^2$ where b_q^\dagger and b_q are creation and annihilation operators. In such notations, the current is written as $j_\alpha = -i\hbar^2 A(\psi^\dagger \partial_\alpha \psi - \psi \partial_\alpha \psi^\dagger)$. Note that Eq. (8) describes charged particles moving in the fictitious electric $\mathcal{E}_\alpha = -\partial_t \mathcal{A}_\alpha^z - \partial_\alpha (\mathcal{A}_0^z + V(\mathbf{r})) = \hbar \tilde{\mathbf{m}}_s \cdot (\partial_t \tilde{\mathbf{m}}_s \times \partial_\alpha \tilde{\mathbf{m}}_s) - \hbar \partial_\alpha V(\mathbf{r})$ and magnetic $\mathcal{B}_i = (\hbar/2) \epsilon^{ijk} \tilde{\mathbf{m}}_s \cdot (\partial_k \tilde{\mathbf{m}}_s \times \partial_j \tilde{\mathbf{m}}_s)$ fields produced by the magnetic texture. In the diffusive regime, the transport of magnons due to such fields can be found by solving the Boltzmann equation within the relaxation-time approximation.

The texture independent transport coefficients can be expressed through the following integrals:

$$\mathcal{J}_n^{\alpha\beta} = \frac{1}{(2\pi)^3 \hbar} \int d\varepsilon \tau(\varepsilon) (\varepsilon - \mu)^n \left(-\frac{\partial f_0}{\partial \varepsilon} \right) \int dS_\varepsilon \frac{v_\alpha v_\beta}{|\mathbf{v}|}, \quad (9)$$

where μ is the chemical potential of magnons, $\tau(\varepsilon)$ is the relaxation time, $\varepsilon(\mathbf{q}) = \hbar\omega_q$, $v_\alpha = \partial\omega_q/\partial q_\alpha$, dS_ε is the area d^2q corresponding to the constant energy $\varepsilon(\mathbf{q}) = \varepsilon$ and $f_0 = \{\exp[(\varepsilon - \mu)/k_B T] - 1\}^{-1}$ is the Bose-Einstein equilibrium distribution. Thus the resistivity tensor is $\rho = \mathcal{J}_0^{-1}$, the analogue of the Peltier coefficient for magnons is $\Pi = -\mathcal{J}_1 \mathcal{J}_0^{-1}$, and the thermal conductivity is $\kappa = (\mathcal{J}_2 - \mathcal{J}_1 \mathcal{J}_0^{-1} \mathcal{J}_1)/T$. The relaxation time τ contains the conserving number of magnons part τ_c , e.g., corresponding to magnon-magnon interactions and disorder scattering, and the nonconserving part, e.g., corresponding to the Gilbert damping τ_α . We can sum up different contributions with different dependence on temperature according to $1/\tau = 1/\tau_c + 1/\tau_\alpha$. In this work, we assume that the scattering is dominated by the Gilbert damping contribution $\tau_\alpha \sim (2\alpha\omega)^{-1}$, where α is the Gilbert damping, which is consistent with our bottom up approach (in some cases, however, the contribution corresponding to the temperature independent scattering length gives better agreement to the experiment [22]). By taking the quadratic spectrum for YIG at room temperature and $\alpha \sim 10^{-3}$ [23], we obtain the mean free path ~ 100 nm from the τ_α relaxation time for magnons.

The above description of magnons contains dissipative β corrections [4] related to a small magnon mistracking of the slow magnetic texture. Such corrections have been extensively studied for charge flows in transition metals and one can use the analogy between the electronic and magnonic systems in order to introduce such corrections into the equations for currents. By following this prescription, one can arrive at Eqs. (4) and (7) with the transport coefficients given by the Boltzmann equation. The coefficient β can then be estimated as $\beta \sim \alpha$ based on the absence of any additional energy scales, apart from the thermal energy, in the low-temperature (compared to the Curie temperature) limit captured by our bottom up approach. More careful estimates of β can be obtained microscopically by solving equation for nonequilibrium spin polarization in the presence of the transverse relaxation [6] or by using the scattering matrix approach [24].

By relating the microscopic description based on Eq.

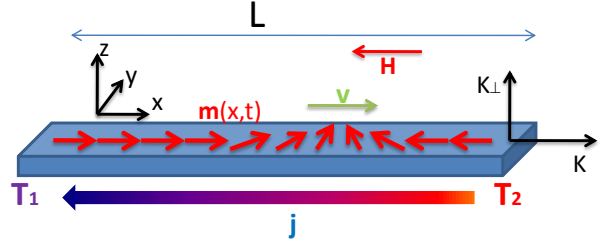


Fig. 2: (Color online) A domain-wall moves towards the hotter end of the wire due to the flow of magnons j . Here, we consider transverse head-to-head Néel domain wall parallel to the y axis in the easy xy plane. The constants K and K_\perp describe the easy axis and easy plane anisotropy.

(7) with Eqs. (4), we can immediately identify some of the kinetic coefficients in Eq. (4), i.e., $p_1 = 0$, $p_1\beta_1 = 0$, $p = -\hbar$ and $\alpha/\beta \sim 1$. Note that p_1 and $p_1\beta_1$ can be nonzero in systems with more than one magnon band and/or added anisotropies. In order to find the remaining coefficients, one could use Boltzmann equation and the relaxation time approximation applied to three dimensional magnons with Bose distribution [e.g., Eq. (9)]. Such description can be further improved by considering the dissipative corrections described by η terms.

Magnonic domain wall motion by temperature gradient. – In this section we show how Eqs. (4) can be used to describe the domain wall motion by employing the Walker ansatz. To this end, we will describe the domain wall in Fig. 2 by the Walker ansatz valid for weak field and current/temperature biases [10, 25]:

$$\varphi(\mathbf{r}, t) \equiv \Phi(t), \quad \ln \tan \frac{\theta(\mathbf{r}, t)}{2} \equiv \frac{x - X(t)}{W(t)}, \quad (10)$$

where the position-dependent spherical angles φ and θ parametrize the magnetic configuration as $\mathbf{m}(x) = m(x)(\cos \theta, \sin \theta \cos \varphi, \sin \theta \sin \varphi)$, $X(t)$ parametrizes the net displacement of the wall along the x axis, and we assume that the driving forces (H , j and j_q) are not too strong so that the wall preserves its shape and only its width $W(t)$ and out-of-plane tilt angle $\Phi(t)$ undergo small changes. By substituting the ansatz (10) in Eq. (7) with the effective field given by $\mathbf{H}_{\text{eff}} = \gamma \mathbf{s} [(H + (\mathbf{s}/s)K m_x) \mathbf{x} - (\mathbf{s}/s)K_\perp m_z \mathbf{z} + (\mathbf{s}/s)A \nabla^2 \mathbf{m}]$, we obtain:

$$\begin{aligned} \dot{\Phi} + \frac{\alpha \dot{X}}{W} &= \gamma H - \frac{p\beta j}{sW}, \\ \frac{\dot{X}}{W} - \alpha \dot{\Phi} &= \frac{\gamma(\mathbf{s}/s)K_\perp \sin 2\Phi}{2} - \frac{pj}{sW}, \\ W &= \sqrt{\frac{A}{K + K_\perp \sin^2 \Phi}}, \end{aligned} \quad (11)$$

where γ is the gyromagnetic ratio, A is the stiffness constant, and K and K_\perp describe the easy axis and easy plane

anisotropies, respectively. Note that the factor \mathfrak{s}/s before the stiffness constant appears due to coarse-graining over fast variables in Eq. (6). This dependence of the effective stiffness constant on the average spin density can lead to additional contribution to the domain wall velocity [30]. In this work, we concentrate on the low temperature limit (on the scale set by the Curie temperature) in which case $\mathfrak{s} \sim s$ and the domain wall motion is dominated by the spin-transfer torque contribution. The steady state solution of Eq. (11) below the Walker breakdown with $\Phi(t) = \text{const}$ and $X = vt$ leads to the result $v = (\gamma HW + \hbar\beta j/s)/\alpha$ or equivalently

$$v = \frac{\gamma W}{\alpha} H + \frac{F_0 \beta}{6\pi^2 \lambda s \alpha} \partial_x T, \quad (12)$$

where λ is the thermal magnon wavelength and we introduce a numerical dimensionless factor $F_0(x) = \int d\epsilon \epsilon^{3/2} e^{\epsilon+x} / (e^{\epsilon+x} - 1)^2 \sim 1$ evaluated at the magnon gap, $x = \hbar\omega_0/k_B T$, which corresponds to dimensionless part of the integral \mathcal{J}_1 in Eq. (9). From Eq. (12), we estimate the domain wall velocity in YIG at room temperature to be 1 cm/sec for the temperature gradient 1 K/ μm .

Peltier effect in quasi-one-dimensional wire. – Peltier effect describes the heat flow accompanying the flow of carriers. Since the moving magnetic texture will induce the flow of magnons, one can discuss the heat currents resulting from such a process. In this section, we concentrate on quasi-one-dimensional systems with a DW propagating in a one dimensional wire connected to two reservoirs in quasi-equilibrium state (Fig. 2). Contrary to the previous sections, the wire can be in the ballistic as well as in the diffusive regime. By writing the equation for the entropy production in the form analogous to the microscopic form in Eq. (3):

$$\dot{S} = \frac{L}{T} \left[-j_q \frac{T_2 - T_1}{TL} - j \frac{\mu_2 - \mu_1}{L} - \dot{X} \frac{2MH}{L} \right], \quad (13)$$

and identifying the thermodynamics variables j_q , j and \dot{X} , we can phenomenologically generalize Eq. (4) to systems possessing domain wall (solitonic) solutions describable by a single generalized coordinate X . The general phenomenological equations for the domain wall dynamics become:

$$\begin{aligned} \dot{X} &= -\mathcal{O}_X(2M_s H/L) - \mathcal{O}_{Xj}\mathcal{E} - \mathcal{O}_{XT}j_q, \\ \mathcal{E}_T/T &= \mathcal{O}_T j_q - \mathcal{O}_{Tj}\mathcal{E} - \mathcal{O}_{XT}(2M_s H/L), \\ j &= \mathcal{O}_j \mathcal{E} + \mathcal{O}_{Tj} j_q + \mathcal{O}_{Xj}(2M_s H/L), \end{aligned} \quad (14)$$

where L is the length of the wire, $\mathcal{E} = -(\mu_2 - \mu_1)/L$, $\mathcal{E}_T = -(T_2 - T_1)/L$ and the kinetic coefficients now correspond to the whole wire, i.e., $\mathcal{O}_T = 1/(\kappa + \kappa ZT)$, $\mathcal{O}_j = 1/(\Upsilon + \Upsilon ZT)$ and $\mathcal{O}_{Tj} = 1/(\Pi + \Pi/ZT)$ with the conventional figure of merit relation for magnons $ZT = \Pi^2/\Upsilon T \kappa$. Using Eq. (14) one can fully describe the interplay between the domain wall motion and magnon/heat currents

in the quasi-one-dimensional systems. The kinetic coefficients can be extracted from the bulk values in the diffusive regime (see below) or can be calculated by scattering theory methods in the ballistic regime [24].

In the following, we analyze the efficiency of heat pumping by a moving domain wall in a system depicted in Fig. 2. Given that the rate of dissipation due to the DW motion in Fig. 2 is $2M_s H \dot{X}$ and it can be assumed to be divided equally between reservoirs, we can calculate the ratio between the useful heat taken from the cooled reservoir and the dissipated heat as the domain wall moves from the left end of the wire to the right end. Such ratios are often calculated in order to characterize thermoelectric circuits [26]. By maximizing the rate of cooling as a function of the domain wall velocity we obtain:

$$COP_{\text{cool}} = \frac{j_q^{\text{cold}}}{2HM\dot{X}} = \frac{T_c}{T_h - T_c} \frac{\sqrt{1 + TZ_{\text{mc}}} - T_h/T_c}{\sqrt{1 + TZ_{\text{mc}}} + 1}. \quad (15)$$

Here j_q^{cold} is the heat current leaving the cooled reservoir and we define the magnetocaloritronic figure of merit [9] by analogy to the thermoelectric figure of merit ZT :

$$TZ_{\text{mc}} = \frac{\mathcal{O}_{XT}^2}{\mathcal{O}_T \mathcal{O}_X}, \quad (16)$$

where we assume that $\mathcal{E} = 0$ and such definition of TZ_{mc} ensures that Eq. (15) is identical to the expression for the thermoelectric COP_{cool} after TZ_{mc} is replaced by ZT . The figure of merit in Eq. (16) is also related to the maximum efficiency of the magnetocaloritronic power generator in a device driven by ac magnetic field [9] contrary to the geometry optimized magnetothermopower in applied dc magnetic field [27]. By taking some particular DW solution we can relate Eqs. (4) with Eqs. (14), e.g., for a transverse head-to-head Néel DW solution in Eq. (10), $\mathcal{O}_X = LW/2\alpha s + \Upsilon(1 + ZT)\mathcal{O}_{Xj}^2$, $\mathcal{O}_{Xj}(1 + ZT) = (p\beta/\Upsilon - p_1\beta_1 ZT/\Pi)/\alpha s$ and $\mathcal{O}_{XT}(1 + ZT) = (p\beta ZT/\Pi + p_1\beta_1/T\kappa)/\alpha s$.

We now estimate TZ_{mc} with $p_1\beta_1 = 0$ according to Eq. (7) and assuming that the scattering is dominated by non-conserving mechanisms described by $\tau_\alpha \sim (2\alpha\omega)^{-1}$. The corresponding mean-free path is assumed to be smaller than the system size in order to ensure the diffusive limit [in principle the ballistic regime can also be treated by Eq. (14) in which the kinetic coefficients should be found using an appropriate microscopic approach]. By invoking Eq. (9) we express the figure of merit as follows:

$$TZ_{\text{mc}} \approx \frac{2F_1\sqrt{k_B T}(\beta/\alpha)^2}{3\pi^2\sqrt{A/\hbar W L s}} \sim \frac{(\beta/\alpha)^2}{W^2\lambda s/\hbar}, \quad (17)$$

where λ is the thermal magnon wavelength, the wire length is taken to be $L \sim W$, and we introduce a numerical dimensionless factor $F_1(x) = [\mathcal{J}_1^2/(\mathcal{J}_0\mathcal{J}_2)] \int d\epsilon \epsilon^{3/2} e^{\epsilon+x} / [(e^{\epsilon+x} - 1)^2(\epsilon + x)]$ evaluated at the magnon gap, $x = \hbar\omega_0/k_B T$, which corresponds to dimensionless part of the ratio $\mathcal{J}_1^2/\mathcal{J}_2$ of integrals in Eq.

(9). We also assume that the domain wall size can be estimated as $W \sim \sqrt{A/\omega_0}$ where ω_0 can be, e.g., the demagnetizing energy. By taking material parameters for YIG at room temperature [28] we arrive at $W \lesssim 100$ nm and $TZ_{\text{mc}} \sim 10^{-4}(\beta/\alpha)^2$, which is quite low. However, larger ratios β/α could be expected as one approaches the Curie temperature. Materials with smaller DW size should be more efficient in heat pumping according to Eq. (17), e.g., we estimate that in EuO $W \sim 1$ nm and $TZ_{\text{mc}} \sim 10^{-3}(\beta/\alpha)^2$ at ~ 10 K using the following parameters: the localized spin $S = 7/2$, the lattice spacing $a_0 = 5.1$ Å and the exchange integral $J_0/k_B \approx 1$ K [29] ($J_0 = a_0 s A / 4 S^2$ for a face-centered lattice). In traditional thermoelectrics ZT plummets to zero much faster than $TZ_{\text{mc}} \propto \sqrt{T}$ in Eq. (17), making magnonic heat pumps promising for cryogenic applications. Furthermore, TZ_{mc} scales as s^{-1} with the spin density thus the dilute magnetic systems (with sufficiently narrow W) should also be suitable for such applications.

To conclude, we developed a phenomenological theory describing magnon and heat currents and the magnetization texture dynamics. Under some simple model assumptions, we are able to extract information about all the phenomenological parameters from the Gilbert damping, the exchange integral, the localized spin and the lattice spacing. The β viscous coupling also appears in our description and is related to the magnon dephasing time. Our estimates show that the viscous coupling effects between magnetization dynamics and magnon flows can be strong in materials with low spin densities and narrow domain walls, which can allow the magnonic manipulation of magnetization dynamics and heat pumping. This opens new prospects for thermomagnonic devices, e.g., thermomagnonic heat pumps and generators, that at low temperatures could effectively compete with traditional thermoelectrics. When resubmitting our manuscript, we became aware of two recent works [30,31] that numerically study the magnonic spin-transfer torque and domain wall motion and arrive at results that are consistent with our studies.

We thank Joseph Heremans and Gerrit E. W. Bauer for useful discussions. This work was supported in part by the Alfred P. Sloan Foundation, DARPA, and NSF under Grant No. DMR-0840965.

REFERENCES

[1] VOLOVİK G. E., *J. Phys. C*, **20** (1987) L83.
 [2] TATARA G., KOHNO H. and SHIBATA J., *Phys. Rep.*, **468** (2008) 213.
 [3] DERY H., DALAL P., CYWINSKI L. and SHAM L. J., *Nature*, **447** (2007) 573; DERY H., WU H., CIFTCIOGLU B., HUANG M., SONG Y., KAWAKAMI R., SHI J., KRIVOROTOV I., ZUTIC I. and SHAM L. J., arXiv:1101.1497.
 [4] ZHANG S. and LI Z., *Phys. Rev. Lett.*, **93** (2004) 127204.

[5] THIAVILLE A., NAKATANI Y., MILTAT J. and SUZUKI Y., *Europhys. Lett.*, **69** (2005) 990.
 [6] TSEKOVNYAK Y., SKADSEM H. J., BRATAAS A. and BAUER G. E. W., *Phys. Rev. B*, **74** (2006) 144405.
 [7] KOHNO H., TATARA G. and SHIBATA J., *J. Phys. Soc. Jpn.*, **75** (2006) 113706.
 [8] DUINE R. A., NUNEZ A. S., SINOVA J. and MACDONALD A. H., *Phys. Rev. B*, **75** (2007) 214420.
 [9] KOVALEV A. A. and TSEKOVNYAK Y., *Phys. Rev. B*, **80** (2009) 100408.
 [10] KOVALEV A. A. and TSEKOVNYAK Y., *Solid State Commun.*, **150** (2010) 500.
 [11] HALS K. M., BRATAAS A. and BAUER G. E., *Solid State Commun.*, **150** (2010) 461.
 [12] SLONCZEWSKI J. C., *J. Magn. Magn. Mater.*, **159** (1996) L1; BERGER L., *Phys. Rev. B*, **54** (1996) 9353.
 [13] HEINRICH B., TSEKOVNYAK Y., WOLTERS DORF G., BRATAAS A., URBAN R. and BAUER G. E. W., *Phys. Rev. Lett.*, **90** (2003) 187601.
 [14] KAJIWARA Y., HARII K., TAKAHASHI S., OHE J., UCHIDA K., MIZUGUCHI M., UMEZAWA H., KAWAI H., ANDO K., TAKANASHI K., MAEKAWA S. and SAITOH E., *Nature*, **464** (2010) 262.
 [15] HATAMI M., BAUER G. E. W., ZHANG Q. and KELLY P. J., *Phys. Rev. Lett.*, **99** (2007) 066603; YU H., GRANVILLE S., YU D. P. and ANSERMET J.-P., *Phys. Rev. Lett.*, **104** (2010) 146601.
 [16] SLONCZEWSKI J. C., *Phys. Rev. B*, **82** (2010) 054403; JIA X., LIU K., XIA K. and BAUER G. E. W., arXiv:1103.3764.
 [17] UCHIDA K., XIAO J., ADACHI H., OHE J., TAKAHASHI S., IEDA J., OTA T., KAJIWARA Y., UMEZAWA H., KAWAI H., BAUER G. E. W., MAEKAWA S. and SAITOH E., *Nat Mater*, **9** (2010) 894.
 [18] ONOSE Y., IDEUE T., KATSURA H., SHIOMI Y., NAGAOSA N. and TOKURA Y., *Science*, **329** (2010) 297.
 [19] LANDAU L. and LIFSHITZ E., *Electrodynamics of Continuous Media* 2nd Edition Vol. 8 (Pergamon, Oxford) 1984.
 [20] GUSLIENKO K. Y., ARANDA G. R. and GONZALEZ J. M., *Phys. Rev. B*, **81** (2010) 014414.
 [21] DUGAEV V. K., BRUNO P., CANALS B. and LACROIX C., *Phys. Rev. B*, **72** (2005) 024456.
 [22] DOUGLASS R. L., *Phys. Rev.*, **129** (1963) 1132.
 [23] HEINRICH B., BURROWES C., MONTOYA E., KARDASZ B., GIRT E., SONG Y.-Y., SUN Y. and WU M., *Phys. Rev. Lett.*, **107** (2011) 066604.
 [24] BAUER G. E. W., BRETZEL S., BRATAAS A. and TSEKOVNYAK Y., *Phys. Rev. B*, **81** (2010) 024427.
 [25] TSEKOVNYAK Y., BRATAAS A. and BAUER G. E., *J. Magn. Magn. Mater.*, **320** (2008) 1282.
 [26] MAHAN G., *Solid State Phys.*, **51** (1997) 81.
 [27] HEREMANS J. P., THRUSH C. M. and MORELLI D. T., *Phys. Rev. Lett.*, **86** (2001) 2098.
 [28] NOVOSELOV K., DUBONOS S., MOROZOV S., HILL E., GRIGORIEVA I. and GEIM A., *J. Low Temp. Phys.*, **139** (2005) 65.
 [29] SÖLLINGER W., HEISS W., LECHNER R. T., RUMPF K., GRANITZER P., KRENN H. and SPRINGHOLZ G., *Phys. Rev. B*, **81** (2010) 155213.
 [30] HINZKE, D. AND NOWAK, U., *Phys. Rev. Lett.*, **107** (2011) 027205.
 [31] YAN, P. AND WANG, X. S. AND WANG, X. R., *Phys.*

Rev. Lett., **107** (2011) 177207.